

Low Temperature Heating of Silver-Mediated Exfoliation of MoS₂

Max Heyl, Sarah Grützmacher, Steffen Rühl, Giovanni Ligorio, Norbert Koch, and Emil J. W. List-Kratochvil*


The need for high-quality large-scale monolayers of layered materials pushes the development of scalable gold-mediated exfoliations. Gold proves to be a suitable adhesive for exfoliation of several 2D materials. However, the extension to other noble metals remains underwhelming as gold outperforms all previously studied metals by a large margin. This is attributed to compromised stability against oxidation and surface contamination of less noble metals, leading to nonideal interfaces for exfoliation. The closest competitor to gold is silver, where gold still leads by a factor 100 regarding exfoliated layer size. In this work, a silver-mediated exfoliation process performing on par with gold is presented. The combination of freshly cleaved silver surfaces with a low-temperature annealing is found to be crucial. The exfoliation yield shows a dependence with annealing temperature, leading to loss in exfoliation performance for higher temperature. Raman studies indicate inhomogeneous strain for the MoS₂/Ag interface at these temperatures, which hints at the competing factors of thermal activation versus oxidation of silver. Finally, a transfer process is implemented to promote silver to a fully functional exfoliation substrate. Ultimately, heating up exfoliations tips the strict balance between interfacial interactions and surface contaminations toward robust high monolayer yield exfoliation as demonstrated for silver.

1. Introduction

To showcase the true potential of 2D materials, mechanical exfoliation has been key to obtain high quality single layers

M. Heyl, S. Grützmacher, S. Rühl, G. Ligorio, E. J. W. List-Kratochvil
Department of Chemistry
Department of Physics & IRIS Adlershof
Humboldt-Universität zu Berlin
Zum Großen Windkanal 2, 12489 Berlin, Germany
E-mail: emil.list-kratochvil@hu-berlin.de

N. Koch
Department of Physics & IRIS Adlershof
Humboldt-Universität zu Berlin
Brook-Taylor-Str. 6, 12489 Berlin, Germany
N. Koch, E. J. W. List-Kratochvil
Helmholtz-Zentrum für Materialien und Energie GmbH
Hahn-Meitner-Platz 1, 14109 Berlin, Germany

 The ORCID identification number(s) for the author(s) of this article can be found under <https://doi.org/10.1002/admi.202200362>.

© 2022 The Authors. Advanced Materials Interfaces published by Wiley-VCH GmbH. This is an open access article under the terms of the Creative Commons Attribution License, which permits use, distribution and reproduction in any medium, provided the original work is properly cited.

DOI: 10.1002/admi.202200362

with a low barrier of entry. While the classical tape-based exfoliation is easy to learn, it is severely limited in terms of scaling.^[1,2] Ideally, not only the high-quality of the starting crystal should be preserved, but also its lateral size is reflected in the exfoliation yield. Here, gold-mediated exfoliations started to shine,^[3–8] where a clean and smooth gold surface provides the necessary interaction to exfoliate a whole array of layered materials.^[4,5] Resulting single layer areas are mostly limited by the parent crystal areas, approaching a near unity exfoliation yield, which allows for large-scale single layers in action.^[3,9–11] The interaction is noncovalent in nature and is highly dependent on the condition of the gold surface, where even slight contamination diminishes the exfoliation yield.^[5] Recently, interfacial strain has been recognized as additional critical factor for the success of gold-mediated exfoliation, promoting the exfoliation of a single layer by disrupting the interlayer stacking.^[12,13] The extension of gold's success to other noble

metals for exfoliation proved to be difficult, as reported previously.^[12] Following a pure binding energy argument with MoS₂ as example, several other noble metals should be able to pull off a similar performance. However, gold remained unchallenged with a two-order of magnitude difference to the next best competitor, silver.^[12] Other metals (e.g., platinum, palladium, and copper) performed even worse.^[12] The poor performance of the metals was attributed to lacking oxidation resistance with reduced metal nobility.^[12] However, silver outperformed platinum and palladium, rendering it an outlier to the described trend. This exception was attributed to a high strain at the MoS₂/Ag interface, due to lattice mismatch. Still, a large strain dispersion hinted at inhomogeneous strain, due to oxidation of the silver interface. It became clear that the two critical factors for successful metal-mediated exfoliation are large interfacial strain applied homogeneously over the interface and cleanliness of the oxide-free metal surface.^[5,12] Balancing these factors is key for high single-layer yield exfoliations, which proved difficult for silver to date. Gold achieves these points by high oxidation resistance and a careful preparation of fresh surfaces prior to exfoliation. One route to obtain metal surfaces suited for this task is the template-strip.^[14,15] A smooth template, e.g., a polished silicon wafer, is covered with a thin layer (≈200 nm) of metal using thermal evaporation. The film can be released

to uncover the pristine and smooth template/metal interface, revealing a fresh exfoliation substrate on demand.^[3,8]

Unlike most gold-mediated exfoliation processes, in our previously reported process a thermal annealing step was key to activate the exfoliation.^[8] This unique characteristic motivated the extension to silver following the discussion of Velický et al.,^[12] by heating up the love affair between MoS₂ and silver to rival gold. In this work, a silver-mediated exfoliation of MoS₂ is presented. Fresh silver surfaces were obtained by a template-strip and exhibited thermally activated exfoliation of MoS₂ with near unity yield. The process was benchmarked against the gold analogue and showed unprecedented performance on par with gold. The temperature dependence of the exfoliation yield was studied and revealed a peak performance ≈150 °C, whereas higher temperature led to a loss in performance, a feature absent for gold. This loss suggests a competing interaction to the thermal activation, likely the oxidation of silver. In this light, Raman studies suggested a more inhomogeneous strain at the MoS₂/Ag interface for higher temperature. X-ray photoelectron spectroscopy (XPS) indicates that at employed temperatures, silver oxidation is effectively suppressed when the metal surface is protected by MoS₂. Lastly, a polymer-based transfer process using polystyrene is implemented to promote silver to a complete exfoliation substrate, with the ability to relocate exfoliated single layers onto target substrates.

2. Results and Discussion

The thermally activated exfoliation with template-strip silver substrates is shown in Figure 1a.

The template-stripped silver substrates are prepared by evaporating a 200 nm silver layer onto a polished silicon wafer. Glass slides for solid support are glued onto the silver-covered wafer surface using UV-curable epoxy. Fresh and smooth silver

surfaces are now available on demand by releasing the silver from the silicon wafer, by using a razor blade. The silver as well as the MoS₂ parent crystal are stripped shortly before exfoliation to maintain both surfaces to be as fresh as possible. Pressing the crystal onto the silver surface followed by some heating leads to exfoliation of MoS₂ on silver. At room temperature no discernible exfoliation occurs, as already observed for gold.^[8] The annealing at 150 °C for 1 min is sufficient to activate exfoliation. Before peeling off the crystal to reveal the exfoliated single layers, a brief precooling step is performed.^[16] The resulting large-scale MoS₂ single layer is directly visible in the optical microscopy image reported in Figure 1b (and zoomed area in Figure 1c). Some multilayers are visible, yet the single layer (1L) areas easily outweigh them with 23 mm² total (≈78% single layer yield). A closer look in Figure 1c reveals a continuous single layer without damage, with a small bilayer (2L) nearby. Atomic force microscopy (AFM) is used to validate the layered nature and is reported in Figure 1d. The measured step height of ≈0.65 nm is in good agreement with the expected MoS₂ interlayer distance.^[17] The 1L-MoS₂/Ag step remained elusive due to the abrupt roughness change (Figure S1, Supporting Information). Overall, the large-scale exfoliation shows results unprecedented for silver, qualifying it as a sustainable and low-cost alternative to gold. It is important to note that this exfoliation works in air despite the previously suggested oxidation of silver being a limiting factor.^[12] The process seems to hit the sweet spot between boosted interfacial interactions and oxidation of silver enabled by the annealing step. Furthermore, the brief duration and low temperature of the annealing step should avoid any material degradation due to defect generations, which are known to occur at temperatures above 200 °C for prolonged time.^[18,19] The large-scale exfoliation was reproducible as well as the near unity single layer yield (Figure S2, Supporting Information). This motivated the extension of this process to copper, a metal with even worse oxidation resistance.

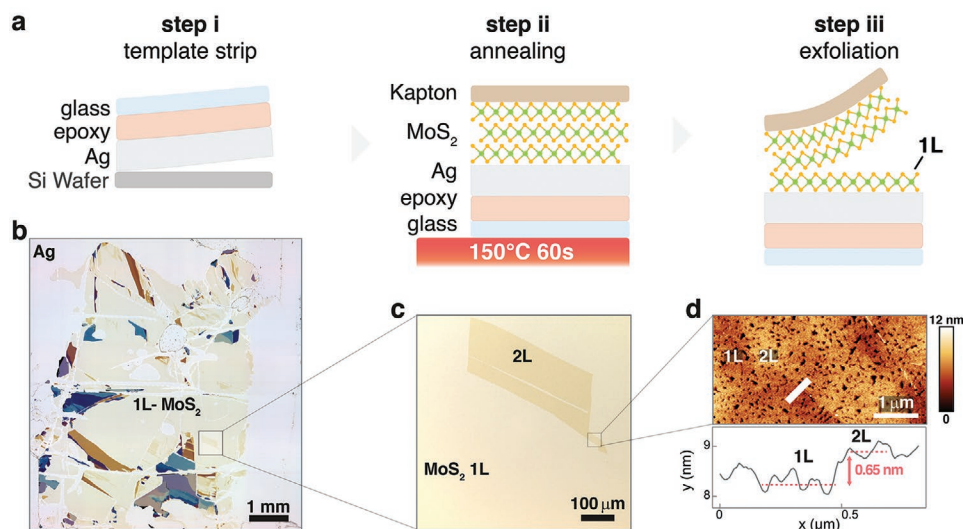


Figure 1. Silver-mediated large-scale exfoliation of MoS₂. a) Schematic of the exfoliation process. Silver is template-stripped (i) and then combined with MoS₂ on heat-resistant Kapton tape to start the annealing (ii) at 150 °C for 60 s. The Kapton tape is used to peel off the MoS₂ crystal (iii), revealing the exfoliated single layer on silver. b) Optical microscopy image of exfoliated MoS₂/Ag. The contrast corresponding to single layer is labelled as 1L-MoS₂. The total 1L-area is 23 mm². c) Zoom-in of the specified position in (b). The single layer region is continuous, and a bilayer (2L) is shown. d) Atomic force microscopy image of the 1L-2L edge highlighted in (c). The step height is ≈0.65 nm.

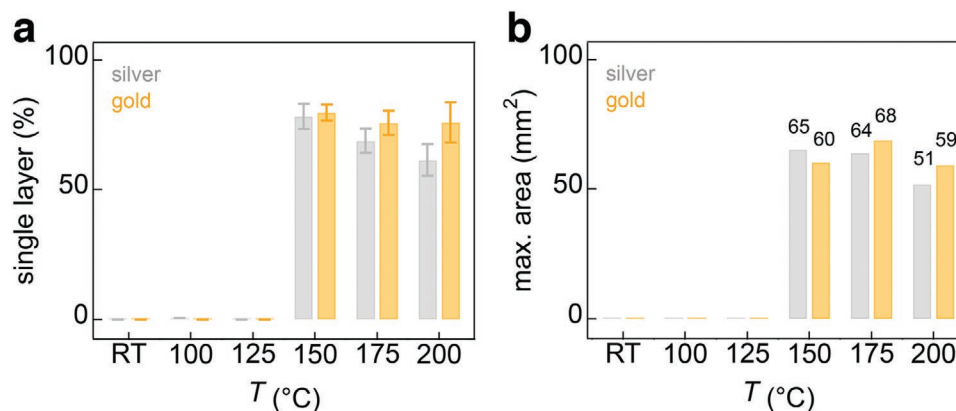


Figure 2. Statistics of silver- and gold-mediated exfoliations of MoS₂ at various temperatures a) Percentage of single layer MoS₂ yield for silver and gold. Without temperature, neither gold nor silver show appreciable exfoliation.^[8] b) Maximum single layer area exfoliated at a given temperature. Maximum areas are labelled above their bars. Silver peaked at 65 mm² at 150 °C, while only achieving 51 mm² at 200 °C. Exfoliation below 150 °C is negligible for both metals. Error bars represent one standard deviation. Sample size *n* for silver/150 °C was 8 and for all others *n* = 4.

However, for copper no exfoliation was observed (Figure S3, Supporting Information).

The silver-mediated exfoliation was benchmarked against gold at several temperatures, as presented in the statistics in **Figure 2**. The single layer yield (Figure 2a) for silver and gold exhibits a temperature dependence with no appreciable continuous single layers exfoliated below 150 °C (Figure S4, Supporting Information). Silver exhibited peak performance at 150 °C and loss in yield for increasing temperature up to 200 °C. For gold, the decrease in performance with increasing temperature is less pronounced. This is consistent with the higher oxidation resistance for gold,^[12] indicating that the loss for silver could be oxidation related. This behaviour is also reflected in the maximum achieved 1L-area (Figure 2b), with multilayer areas in Figure S5, Supporting Information), which again peak at 150 °C for silver, while for gold no significant change is observed between 150 and 200 °C. Furthermore, the statistics clearly show that silver is capable to perform on the same level as gold with the added heat in this procedure. When compared to previous reports, where silver exfoliation size was 1/100 that of gold,^[12] it becomes evident that the presented procedure dramatically increases the exfoliation performance of silver. The otherwise strict process conditions are relaxed upon annealing, potentially due to surface reconstructions of silver at the MoS₂/Ag interface. The restructuring of silver or gold at the MoS₂ interface due to annealing can be rationalized by the hopping barrier (E_{hop}) experienced by metal adatoms on MoS₂, which was previously reported for gold (39 meV) and silver (49 meV).^[20] Increasing thermal energy from room temperature (26 meV) to 150 or 200 °C increases thermal energy to ≈36 and 41 meV, respectively, which enables both metals to restructure accordingly at the MoS₂ interface during exfoliation. This allows to bypass otherwise strict cleanliness requirements by reforming parts of the metal/MoS₂ interface, as indicated in Figure 1d exhibiting regions with intimate contact of silver with MoS₂ and holes in-between.

To elucidate the role of interfacial strain, Raman studies were conducted (**Figure 3a**). The peak position shift of the E^2_{1g} mode relative to SiO₂ indicates tensile straining of MoS₂ on gold and silver.^[12,21] The shape of this mode hints at a strain distribution,

where for silver the more asymmetric and broadened E^2_{1g} mode suggests a wider strain distribution compared to gold, consistent with previous work.^[12] The shift of the E^2_{1g} mode was used to estimate the strain,^[21] using E^2_{1g} peak positions obtained from Voigt fits (see Figure 3a). For MoS₂ exfoliated on gold, a strain of ≈0.7% is observed, where a single component almost suffices to fit the E^2_{1g} mode. For MoS₂ on silver exfoliated at 150 °C, two components are necessary, and the high-strain feature ≈ 2% strain seems even more pronounced at 200 °C. This indicates an increase in the strain inhomogeneity in MoS₂ (Figure S6, Supporting Information), consistent with increased oxidation of silver. Another factor for increased strain

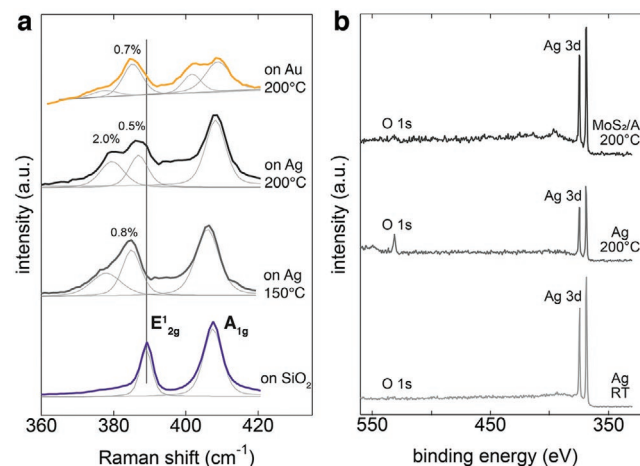


Figure 3. Raman and photoelectron spectroscopy study of the MoS₂-metal interface. a) Raman spectroscopy for strain analysis of single layer MoS₂ on gold, silver, and SiO₂. The strain is derived from the E^2_{1g} peak position relative to the position on SiO₂.^[12,21] Strain values of the E^2_{1g} modes on different metals are indicated. Voigt curve fits are used to determine peak positions and are indicated as grey lines. For silver, two peaks are visible, which is even more apparent for 200 °C. b) X-ray photoelectron spectroscopy survey of the MoS₂/Ag interface, annealed silver surface and pristine template-stripped silver (Ag RT). The increase of the O 1s peak indicates oxidation for annealed silver in air, which is suppressed at the MoS₂/Ag interface.

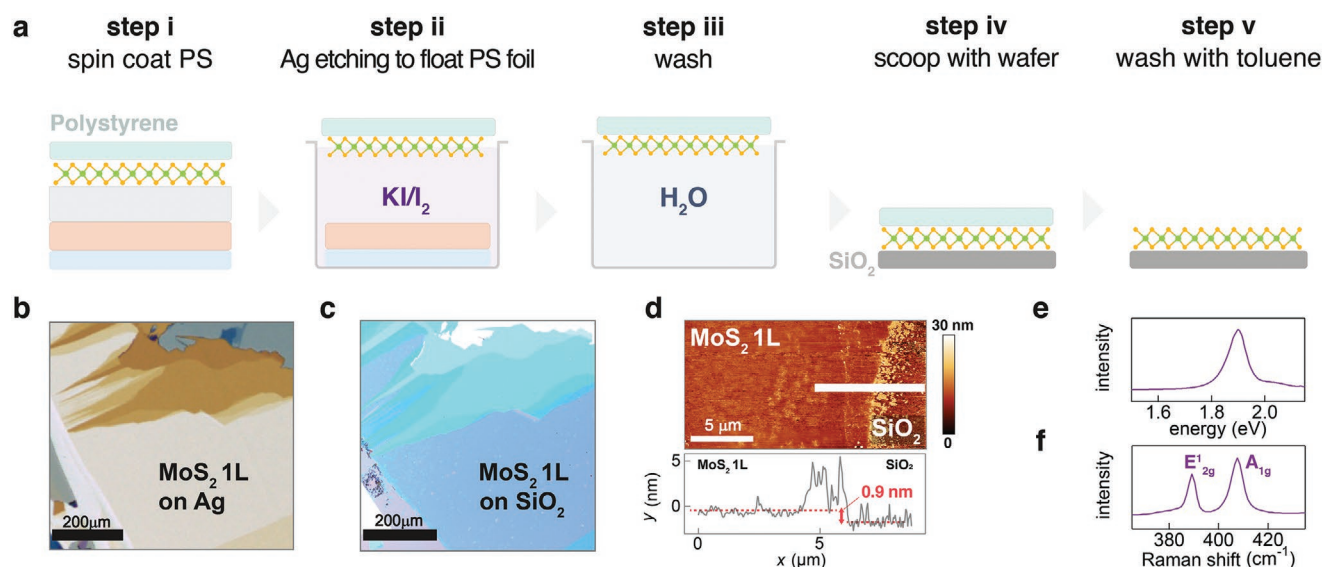


Figure 4. Polystyrene-based transfer of silver-exfoliated MoS₂. a) Schematic of the transfer process. b,c) Before and after optical micrograph of MoS₂ on Ag and transferred onto SiO₂. d) MoS₂ single layer step height on SiO₂ after transfer determined by AFM. The step height is circa 0.9 nm.^[24] e) Photoluminescence spectrum of transferred 1L-MoS₂.^[25] f) Raman spectroscopy of the transferred single layer. The A_{1g}-E_{2g} distance equals to 18.3 cm⁻¹, as expected for a single layer.^[27,28] The E_{1g} peak is well defined, compared to the strain-broadened peak on silver.

inhomogeneity could be related to the distinct growth morphologies of gold and silver on MoS₂. Gold has been reported to cluster into ordered nanostructures, where silver showed more random clusters.^[20,22] This would explain the presence of a high strain component on Au (Figure 3a) due to cluster formation. Consequently, larger strain broadening is expected for the more random clustering at the MoS₂/Ag interface.

The finding that gold strains MoS₂ more homogeneously is consistent with previous reports, where it was attributed to the oxide-free gold surface.^[12] This might explain the loss in exfoliation performance for higher temperature due to oxidation of silver. XPS was used to study the MoS₂/Ag interface in more detail and the survey scans are shown in Figure 3b. Freshly evaporated silver does not display a notable peak corresponding to the presence of oxygen, i.e., silver oxidation. For silver annealed at 200 °C in air, pronounced oxidation is indicated by the increased O 1s peak. This is not the case for the sample with MoS₂ on silver. This indicates that at 200 °C the oxidation of silver is strongly suppressed once the metallic surface is passivated by the MoS₂.

With large scale single layers on silver, the next step is to transfer these onto arbitrary substrates. Hence, a polystyrene-based transfer was adopted^[23] and implemented (Figure 4a). All features remained unchanged, as seen in Figure 4b,c, indicating a deterministic transfer process. AFM revealed a 1L-MoS₂/SiO₂ step height of ≈0.9 nm, consistent with previous work.^[8,24] The photoluminescence spectrum (Figure 4d) highlights the characteristic direct bandgap emission for an intact single layer.^[25] Notably, the previously strained MoS₂ on silver shows a narrow and symmetric E_{2g}¹ mode on SiO₂ after transfer (Figure 4e), indicating effective strain release.^[26] With the transfer implemented, silver serves as a fully functioning exfoliation substrate.

3. Conclusion

In conclusion, heating up the silver-mediated exfoliation dramatically increases the exfoliation performance by tipping the strict balance of process conditions, i.e., interfacial interactions and surface contaminations, toward a high single layer yield exfoliation process. The combination of fresh template-stripped silver and the low temperature annealing enables unprecedented performance on par with gold. A temperature dependence of the exfoliation yield is observed, suggesting a thermally activated process limited by oxidation for higher temperatures. Thereby, this work highlights the importance of temperature as a key parameter in metal-mediated exfoliation to enhance process robustness and performance.

4. Experimental Section

Metal Exfoliation Substrates: Silicon wafers (Siegert Wafer, <100>, 525 μm thickness) served as the templates. 200 nm Au or Ag were deposited via physical vapor deposition (≈1.0 Å s⁻¹ at 10⁻⁶mbar). Glass chips were fixed onto the metal coated wafer with UV-curable epoxy resin (Ossila Encapsulation Epoxy S132).

Metal-Assisted Exfoliation: MoS₂ (2D semiconductors, synthetic MoS₂ crystal) was cleaved with heat-resistant Kapton tape and pressed onto the freshly template-stripped metal substrate. Then the annealing step followed on a hotplate in ambient conditions at the temperatures described in the main text for 60 s, followed by a cool down by removing the substrate from the hotplate and waiting for ≈15 s before peeling the tape.

Polystyrene-Assisted Transfer: MoS₂ on Ag was transferred with polystyrene adapting a reported process.^[23] Polystyrene was spin coated (Sigma-Aldrich, average M_w ≈ 280.000, 90 mg mL⁻¹ in toluol, 3000 rpm 60 s) onto the MoS₂/Ag substrate and annealed at 80 °C for 10 min. The sample was left on the KI/I₂ (Sigma-Aldrich) metal-etchant until the polystyrene foil floated on top (≈12 h). The foil was fished out with a clean wafer piece and transferred into a beaker with deionized water to clean off etchant residues. The foil was transferred into a beaker with

fresh DI H₂O and fished out with the target substrate. The sample was dried in air for 12 h before baking on a hotplate (80 °C 1 h, 150 °C 30 min). To release the MoS₂ on the target, the polystyrene was removed with hot (90 °C) toluene followed by washing with acetone and isopropyl alcohol.

AFM Measurements: AFM was performed in air with a Bruker Dimension Icon using PeakForce Tapping with a ScanAsyst-Air tip (Bruker).

Raman and Photoluminescence Measurements: Raman and PL spectroscopy were performed using a confocal microscope setup (XploRA, Horiba Ltd.) with 532 nm laser excitation source and 100× objective (≈1 μm laser spot size) using a 2400 L mm⁻¹ grating for Raman and 600 L mm⁻¹ for PL. The measurements were conducted in ambient conditions.

X-Ray Photoelectron Spectroscopy: XPS spectra were acquired on the JEOL JPS-9030 photoelectron spectrometer system. As excitation source, monochromatic Al Kα (1486 eV) was employed. The sample was grounded during the spectra acquisition.

Statistical Analysis: The data of single layer yield and maximum single area (Figure 2) were used without further pre-processing. In this data presentation the mean value was represented by the bar height and the standard deviation (±SD) is given as error bar. The sample size *n* was 4 for all temperature/metal pairs but 150 °C/Ag, where *n* = 8. To measure the exfoliated areas, optical micrograph images were analyzed in the Gwyddion software. For silver the blue channel of the RGB image was used for the best contrast while for gold the green channel was the best. Monolayer areas were detected and measured by threshold detection as implemented in Gwyddion. For the statistical analysis, the Igor Pro software was used.

Supporting Information

Supporting Information is available from the Wiley Online Library or from the author.

Acknowledgements

The authors would like to acknowledge Paul Zybarth and Bodo Kranz for their continuous support in the lab. Furthermore, the authors would like to acknowledge Felix Hermerschmidt for careful proof reading of the manuscript. The authors gratefully acknowledge financial support by the Deutsche Forschungsgemeinschaft through CRC 951 (Project number 182087777). This work was carried out in the framework of the Joint Lab GEN_FAB and was supported by the HySPRINT Innovation Lab at Helmholtz-Zentrum Berlin.

Open access funding enabled and organized by Projekt DEAL.

Conflict of Interest

The authors declare no conflict of interest.

Data Availability Statement

The data that support the findings of this study are available in the supplementary material of this article.

Keywords

annealing, exfoliation of 2D materials, MoS₂, silver, thermally activated exfoliation, TMDCs

Received: February 24, 2022

Revised: April 7, 2022

Published online: May 20, 2022

- [1] K. S. Novoselov, D. Jiang, F. Schedin, T. J. Booth, V. v Khotkevich, S. v Morozov, A. K. Geim, *Proc. Natl. Acad. Sci. USA* **2005**, *102*, 10451.
- [2] K. S. Novoselov, A. K. Geim, S. v Morozov, D. Jiang, Y. Zhang, S. v Dubonos, I. v Grigorieva, A. A. Firsov, *Science* **2004**, *306*, 666.
- [3] L. Fang, W. Wenjing, B. Yusong, C. S. Hoon, L. Qiuyang, W. Jue, H. James, X.-Y. Zhu, *Science* **2020**, *367*, 903.
- [4] Y. Huang, Y.-H. Pan, R. Yang, L.-H. Bao, L. Meng, H.-L. Luo, Y.-Q. Cai, G.-D. Liu, W.-J. Zhao, Z. Zhou, L.-M. Wu, Z.-L. Zhu, M. Huang, L.-W. Liu, L. Liu, P. Cheng, K.-H. Wu, S.-B. Tian, C.-Z. Gu, Y.-G. Shi, Y.-F. Guo, Z. G. Cheng, J.-P. Hu, L. Zhao, G.-H. Yang, E. Sutter, P. Sutter, Y.-L. Wang, W. Ji, X.-J. Zhou, et al, *Nat. Commun.* **2020**, *11*, 2453.
- [5] M. Velický, G. E. Donnelly, W. R. Hendren, S. McFarland, D. Scullion, W. J. I. DeBenedetti, G. C. Correa, Y. Han, A. J. Wain, M. A. Hines, D. A. Muller, K. S. Novoselov, H. D. Abruña, R. M. Bowman, E. J. G. Santos, F. Huang, *ACS Nano* **2018**, *12*, 10463.
- [6] S. B. Desai, S. R. Madhvapathy, M. Amani, D. Kiriya, M. Hettick, M. Tosun, Y. Zhou, M. Dubey, J. W. Ager III, D. Chrzan, A. Javey, *Adv. Mater.* **2016**, *28*, 4053.
- [7] G. Z. Magda, J. Pető, G. Dobrik, C. Hwang, L. P. Biró, L. Tapasztó, *Sci. Rep.* **2015**, *5*, 14714.
- [8] M. Heyl, D. Burmeister, T. Schultz, S. Pallasch, G. Ligorio, N. Koch, E. J. W. List-Kratochvil, *Phys. Status Solidi Rapid Res. Lett.* **2020**, *14*, 2000408.
- [9] H. M. Gramling, C. M. Towle, S. B. Desai, H. Sun, E. C. Lewis, V. D. Nguyen, J. W. Ager, D. Chrzan, E. M. Yeatman, A. Javey, H. Taylor, *ACS Appl. Electron. Mater.* **2019**, *1*, 407.
- [10] S. Rühl, M. Heyl, F. Gärisch, S. Blumstengel, G. Ligorio, E. J. W. List-Kratochvil, *Phys. Status Solidi Rapid Res. Lett.* **2021**, *15*, 2100147.
- [11] S. Dalgleish, L. Reissig, Y. Shuku, G. Ligorio, K. Awaga, E. J. W. List-Kratochvil, *Sci. Rep.* **2019**, *9*, 16682.
- [12] M. Velický, G. E. Donnelly, W. R. Hendren, W. J. I. DeBenedetti, M. A. Hines, K. S. Novoselov, H. D. Abruña, F. Huang, O. Frank, *Adv. Mater. Interfaces* **2020**, *7*, 2001324.
- [13] H. Sun, E. W. Sirott, J. Mastandrea, H. M. Gramling, Y. Zhou, M. Poschmann, H. K. Taylor, J. W. Ager, D. C. Chrzan, *Phys. Rev. Mater.* **2018**, *2*, 94004.
- [14] N. Vogel, J. Zieleniecki, I. Köper, *Nanoscale* **2012**, *4*, 3820.
- [15] M. Hegner, P. Wagner, G. Semenza, *Surf. Sci.* **1993**, *291*, 39.
- [16] Y. Zhang, X. Chen, H. Zhang, S. Hu, G. Zhao, M. Zhang, W. Qin, Z. Wang, X. Huang, J. Wang, *Front. Chem.* **2021**, *9*, 650901.
- [17] B. Radisavljevic, A. Radenovic, J. Brivio, V. Giacometti, A. Kis, *Nat. Nanotechnol.* **2011**, *6*, 147.
- [18] D. M. Sim, M. Kim, S. Yim, M.-J. Choi, J. Choi, S. Yoo, Y. S. Jung, *ACS Nano* **2015**, *9*, 12115.
- [19] M. Donarelli, F. Bisti, F. Perrozzi, L. Ottaviano, *Chem. Phys. Lett.* **2013**, *588*, 198.
- [20] C. Gong, C. Huang, J. Miller, L. Cheng, Y. Hao, D. Cobden, J. Kim, R. S. Ruoff, R. M. Wallace, K. Cho, X. Xu, Y. J. Chabal, *ACS Nano* **2013**, *7*, 11350.
- [21] D. Lloyd, X. Liu, J. W. Christopher, L. Cantley, A. Wadehra, B. L. Kim, B. B. Goldberg, A. K. Swan, J. S. Bunch, *Nano Lett.* **2016**, *16*, 5836.
- [22] Y. A. Moe, Y. Sun, H. Ye, K. Liu, R. Wang, *ACS Appl. Mater. Interfaces* **2018**, *10*, 40246.
- [23] A. Gurarlan, Y. Yu, L. Su, Y. Yu, F. Suarez, S. Yao, Y. Zhu, M. Ozturk, Y. Zhang, L. Cao, *ACS Nano* **2014**, *8*, 11522.
- [24] Z. Zeng, Z. Yin, X. Huang, H. Li, Q. He, G. Lu, F. Boey, H. Zhang, *Angew. Chem.* **2011**, *123*, 11289.
- [25] K. F. Mak, C. Lee, J. Hone, J. Shan, T. F. Heinz, *Phys. Rev. Lett.* **2010**, *105*, 2.
- [26] Z. Liu, M. Amani, S. Najmaei, Q. Xu, X. Zou, W. Zhou, T. Yu, C. Qiu, A. G. Birdwell, F. J. Crowne, R. Vajtai, B. I. Yakobson, Z. Xia, M. Dubey, P. M. Ajayan, J. Lou, *Nat. Commun.* **2014**, *5*, 5246.
- [27] H. Li, Q. Zhang, C. C. R. Yap, B. K. Tay, T. H. T. Edwin, A. Olivieri, D. Baillargeat, *Adv. Funct. Mater.* **2012**, *22*, 1385.
- [28] C. Lee, H. Yan, L. E. Brus, T. F. Heinz, J. Hone, S. Ryu, *ACS Nano* **2010**, *4*, 2695.